

BRAIN ANATOMICAL FEATURE DETECTION BY SOLVING PARTIAL DIFFERENTIAL EQUATIONS ON GENERAL MANIFOLD

LOK MING LUI¹, YALIN WANG^{1,2}, TONY F. CHAN¹ AND PAUL M. THOMPSON²

¹ Department of Mathematics, UCLA
Los Angeles, CA 90095-1555, USA

² Laboratory of Neuro Imaging
Dept. of Neurology, UCLA School of Medicine
Los Angeles, CA 90095, USA

ABSTRACT. One important problem in the human brain mapping research is to locate the important anatomical features. Anatomical features on the cortical surface are usually represented by landmark curves, called sulci/gyri curves. These landmark curves are important information for neuroscientists to study brain disease and to match different cortical surfaces. Manual labelling of these landmark curves is time-consuming, especially when large sets of data have to be analyzed. In this paper, we present algorithms to automatically detect and match landmark curves on cortical surfaces to get an optimized brain conformal parametrization. First, we propose an algorithm to obtain a hypothesized landmark region/curves using the Chan-Vese segmentation method, which solves a Partial Differential Equation (PDE) on a manifold with global conformal parameterization. This is done by segmentating the high mean curvature region. Second, we propose an automatic landmark curve tracing method based on the principal directions of the local Weingarten matrix. Based on the global conformal parametrization of a cortical surface, our method adjusts the landmark curves iteratively on the spherical or rectangular parameter domain of the cortical surface along its principal direction field, using umbilic points of the surface as anchors. The landmark curves can then be mapped back onto the cortical surface. Experimental results show that the landmark curves detected by our algorithm closely resemble these manually labeled curves. Next, we applied these automatically labeled landmark curves to generate an optimized conformal parametrization of the cortical surface, in the sense that homologous features across subjects are caused to lie at the same parameter locations in a conformal grid. Experimental results show that our method can effectively help in automatically matching cortical surfaces across subjects.

1. Introduction. Finding feature points or curves in medical images is an important problem in medical imaging. For example, anatomical features on the cortical surface can be represented by landmark curves, called sulci/gyri curves. These sulci/gyri curves are important information for neuroscientists to study brain disease and to match different cortical surfaces. It is time-consuming to label these landmark curves manually, especially when there are large sets of data. Therefore, an automatic or semi-automatic way to detect these feature curves is necessary.

2000 *Mathematics Subject Classification.* Primary: 58F15, 58F17; Secondary: 53C35.

Key words and phrases. Brain Anatomical Feature, Conformal Parametrization, Partial Differential Equations, Variational problem, Curvature.

In this paper, we trace the landmark curves on the cortical surfaces automatically based on the principal directions. Suppose we are given the global conformal parametrization of the cortical surface. Fixing two endpoints, called the anchor points, we trace the landmark curve iteratively on the spherical/rectangular parameter domain along one of the two principal directions. Consequently, the landmark curves can be mapped onto the cortical surface. To speed up the iterative scheme, a good initial guess of the landmark curve is necessary. Therefore, we propose a method to get a good initialization by extracting the high curvature region on the cortical surface using Chan-Vese segmentation [1]. This involves solving a PDE (Euler-Lagrange equation) on the manifold using the global conformal parametrization. As an application, we used these automatic labelled landmark curves to get an optimized brain conformal mapping, which can match important anatomical features across subjects. This is based on the minimization of a combined energy $E_{new} = E_{harmonic} + \lambda E_{landmark}$. Our paper is organized as follows: the basic mathematical theory will be discussed in section 2. The computational algorithm of the conformal parameterization and curvature matrix will be discussed in sections 3 and 4. In sections 5 and 6, the algorithm of the automatic landmark tracking and its application to the optimization of brain conformal mapping will be discussed. The experimental results will be studied in section 7. Finally, the conclusion and future works will be discussed in section 8.

1.1. Previous work. Automatic detection of sulci landmarks on the brain has been widely studied by different research groups. Prince et al. [2] has proposed a method for automated segmentation of major cortical sulci on the outer brain boundary. This is based on a statistical shape model, which includes a network of deformable curves on the unit sphere, seeks geometric features such as high curvature regions, and labels such features via a deformation process that is confined within a spherical map of the outer brain boundary. Lohmann et al. [3] has proposed an algorithm that automatically detects and attributes neuroanatomical names to the cortical folds using image analysis methods applied to magnetic resonance data of human brains. The sulci basins are segmented using a region growing approach. Zeng et al. [4] has proposed a method to automate intrasulcal ribbon finding, by using the cortex segmentation with coupled surfaces via a level set methods, where the outer cortical surface is embedded as the zero level set of a high-dimensional distance function. Recently, Kao et al. [5] present a sequence of geometric algorithms to automatically extract the sulcal fundi and represent them as smooth polylines lying on the cortical surface. Based on geodesic depth information, their algorithm extracts sulcal regions by checking the connectivity above some depth threshold. After extracting endpoints of the fundi and then thinning each connected region with fixed endpoints, the curves are then smoothed using weighted splines on surfaces.

Optimization of surface diffeomorphisms by landmark matching has been studied intensively. Gu et al. [?] proposed to optimize the conformal parametrization by composing an optimal Möbius transformation so that it minimizes the landmark mismatch energy. The resulting parameterization remains conformal. Wang et al. [7] proposed a new framework that combines genus zero surface conformal mapping with some explicit geometric feature based constraints. The framework has the advantages that the constrain energy is dramatically reduced while the map's conformality is significantly preserved. Joan et al. [8] proposed to generate large deformation diffeomorphisms of the sphere onto itself, given the displacements of a

finite set of template landmarks. The diffeomorphism obtained can match the geometric features significantly but it is, in general, not a conformal mapping. Leow et al. [?] proposed a level set based approach for matching different types of features, including points and 2D or 3D curves represented as implicit functions. Cortical surfaces were flattened to the unit square. Nine sulcal curves were chosen and represented by the intersection of two level set functions. They were used to constrain the warp of one cortical surface onto another. The resulting transformation was interpolated using a large deformation momentum formulation in the cortical parameter space, generalizing an elastic approach for cortical matching developed in Thompson et al. [10].

2. Basic mathematical theory. Firstly, a diffeomorphism $\phi : M \rightarrow N$ is a *conformal mapping* if it preserves the first fundamental form up to a scaling factor (the conformal factor). Mathematically, this means that $ds_M^2 = \lambda \phi^*(ds_N^2)$, where ds_M^2 and ds_N^2 are the first fundamental form on surfaces M and N , respectively and λ is the conformal factor [?].

Next, the normal curvature κ_n of a Riemann surface in a given direction is the reciprocal of the radius of the circle that best approximates a normal slice of the surface in that direction, which varies in different directions. It follows that: $\kappa_n = \mathbf{v}^T \mathbb{III} \mathbf{v} = \mathbf{v}^T \begin{pmatrix} e & f \\ f & g \end{pmatrix} \mathbf{v}$ for any tangent vector \mathbf{v} . \mathbb{III} is called the Weingarten matrix and is symmetric. Its eigenvalues and eigenvectors are called *principal curvatures* and *principal directions* respectively. The mean of the eigenvalues is the *mean curvature*. A point on the Riemann surface at which the Weingarten matrix has the same eigenvalues is called an *umbilic point* [12].

3. Computation of conformal parameterization. It is well known that any genus zero Riemann surfaces can be mapped conformally to a sphere. For the diffeomorphism between two genus zero surfaces, we can get a conformal map by minimizing the harmonic energy [?]. By setting the zero of mass constraint, there exists a unique conformal mapping up to Möbius transformation. For high genus surfaces, Gu and Yau [13] proposed an efficient approach to parameterize surfaces conformally using a set of connected 2D rectangles. They compute a holomorphic 1-form on the Riemann surface, using concepts from homology and cohomology group theory, and Hodge theory. (See Figure 1 left [?]). We can summarize the algorithm with the following five steps (For details, please refer to [13]):

Step 1: Given a high genus surface, find the homology basis $\{\xi_1, \dots, \xi_{2g}\}$ of its homology group.

Step 2: Given the homology basis $\{\xi_1, \dots, \xi_{2g}\}$, compute its dual basis $\{w_1, \dots, w_{2g}\}$ which is called the cohomology basis.

Step 3: Diffuse the cohomology basis elements to harmonic 1-forms. This can be done by solving the following simultaneous equations:

$$(1) dw = 0 \text{ (closedness)} \quad (2) \Delta w = 0 \text{ (harmonicity)} \quad (3) \int_{\xi_i} w_j = \delta_{ij} \text{ (duality)}$$

The existence of solution is guaranteed by Hodge theory.

Step 4: Compute the Hodge star conjugate $\{^*w_1, \dots, ^*w_{2g}\}$ of $\{w_1, \dots, w_{2g}\}$

Step 5: Integrate the holomorphic 1-form and get the conformal mapping: $\phi(x) = \int_{\gamma} w + i^*w$, where $w = \sum \lambda_i w_i$

The above five steps allow us to compute a conformal parametrization from the surface onto the 2D domain.

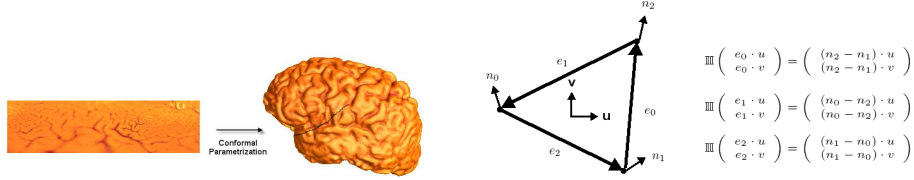


FIGURE 1. Left: Global conformal parametrization of the entire cortical surface onto the 2D rectangle. By introducing cutting boundaries on the cortical surface, the genus of the surface is increased. Holomorphic 1-form and the conformal parametrization can be found. The boundaries of the rectangle corresponds to the cutting boundaries on the surface. Right: A single face (triangle) of the triangulated mesh.

TABLE 1. Illustrates a list of formulas for some standard differential operators on a general manifold.

1. $\nabla_M f = \sum_{i,j} g^{ij} \partial_j f \partial_i$, where (g^{ij}) is the inverse of the Riemannian metric (g_{ij}) . With the conformal parametrization ϕ , the conformal factor λ ,

$$\nabla_M f = D_x f \mathbf{i} + D_y f \mathbf{j},$$
 where $(\mathbf{i}, \mathbf{j}) = (\frac{\partial}{\partial x} / \sqrt{\langle \frac{\partial}{\partial x}, \frac{\partial}{\partial x} \rangle}, \frac{\partial}{\partial y} / \sqrt{\langle \frac{\partial}{\partial y}, \frac{\partial}{\partial y} \rangle})$

$$= \frac{1}{\sqrt{\lambda}} (\frac{\partial}{\partial x}, \frac{\partial}{\partial y}).$$
2. Suppose $h : M \rightarrow \mathbb{R}$ is a smooth function,
 Length of $h^{-1}(0) = \int_M \delta(h) \sqrt{\langle \nabla_M h, \nabla_M h \rangle} dS$

$$= \int_M \sqrt{\langle \nabla_M H(h), \nabla_M H(h) \rangle} dS$$

$$= \int_C \delta(h \circ \phi) \sqrt{\lambda} \|\nabla h \circ \phi\| dx dy$$

$$= \int_C \sqrt{\lambda} \|\nabla H(h \circ \phi)\| dx dy$$
 where H is the Heaviside function.
3. For differential operator on vector field, the covariant derivative satisfies the following properties:
 (P1) $\nabla_f X_1 + g X_2 Y = f \nabla_{X_1} Y + g \nabla_{X_2} Y$ for $f, g \in C^\infty(M)$;
 (P2) $\nabla_X (aY_1 + bY_2) = a \nabla_X Y_1 + b \nabla_X Y_2$, $a, b \in \mathbb{R}$;
 (P3) $\nabla_X (fY) = f \nabla_X Y + (Xf)Y$ for $f \in C^\infty(M)$.
 Suppose $\{\partial_i\}$ is the coordinate basis of the vector field, then

$$\langle \nabla_{\partial_i} \partial_j, \partial_l \rangle = 1/2 (\partial_i g_{jl} + \partial_j g_{li} - \partial_l g_{ij}),$$

$$\nabla_{\partial_i} \partial_j = \Gamma_{ij}^m \partial_m,$$
 where $\Gamma_{ij}^m = \frac{1}{2\lambda} (\partial_i g_{jm} + \partial_j g_{mi} - \partial_m g_{ij})$.
4. For the divergence and Laplacian, we have

$$\text{div}_M (\sum_{i=1}^2 X_i \frac{\partial}{\partial x_i}) = \sum_{i=1}^2 \frac{1}{\lambda} \partial_i (X_i \lambda),$$

$$\Delta_M f = \sum_{j=1}^2 (1/\lambda) \partial_j \partial_j f.$$
5. Suppose C is a curve represented by the zero level set of $\phi : M \rightarrow \mathbb{R}$,
Geodesic curvature of $C = \text{div}_M (\frac{\nabla_M \phi}{\|\nabla_M \phi\|})$.

4. Solving PDEs on surfaces using the global conformal parameterization. We propose to solve PDEs on surfaces by using the global conformal parametrization. The main idea is to map the surface conformally to the 2D rectangles with the minimum number of coordinates patches. The problem can then be solved by solving a modified PDE on the 2D parameter domain. To do this, we have to use a set of differential operators on the manifold, namely, the covariant derivative. With the conformal parametrization, the covariant derivative can be formulated easily with simple formulas on the parameter domains (See Table 1). Once the PDE on the 3D surface is reformulated to the corresponding PDE on the 2D domain, we can solve the PDE on 2D by using some well-known numerical schemes. Since the Jacobian of the conformal mapping is simply a multiplication of the conformal factor, the modified PDE on the parameter domain will be very simple and easy to solve.

5. Algorithm for automatic landmark tracking. In this section, we discuss our algorithm for automatic landmark tracking.

5.1. Computation of principal direction fields from the global conformal parametrization. Denote the cortical surface by C . Let $\phi : D \rightarrow C$ be the global conformal parametrization of C where D is a rectangular parameter domain. Let λ be the conformal factor of ϕ . Similar to Rusinkiewicz's work [15], we can compute the principal directions, and represent them on the parameter domain D . This is based on the following three steps:

Step 1 : Per – Face Curvature Computation

Let $u = \begin{pmatrix} \frac{1}{\sqrt{\lambda}} \\ 0 \end{pmatrix}$ and $v = \begin{pmatrix} 0 \\ \frac{1}{\sqrt{\lambda}} \end{pmatrix}$ be the directions of an orthonormal coordinate system for the tangent plane (represented in the parameter domain D). We can approximate the Weingarten matrix \mathbb{III} for each face (triangle). For a triangle with three well-defined directions (edges) together with the differences in normals in those directions (Refer to Figure 1 right), we have a set of linear constraints on the elements of the Weingarten matrix, which can be determined using the least square method.

Step 2 : Coordinate system Transformation

After we have computed the Weingarten matrix on each face in the (u_f, v_f) coordinate system, we can average it with contribution from adjacent triangles. Suppose that each vertex p has its own orthonormal coordinate system (u_p, v_p) . We have to transform the Weingarten matrix tensor into the vertex coordinates frame. The first component of \mathbb{III} , expressed in the (u_p, v_p) coordinate system, can be found as:

$$e_p = u_p^T \mathbb{III} u_p = (1, 0) \begin{pmatrix} e_p & f_p \\ f_p & g_p \end{pmatrix} (1, 0)^T$$

Thus,

$$e_p = (u_p \cdot u_f, u_p \cdot v_f) \mathbb{III} (u_p \cdot u_f, u_p \cdot v_f)^T$$

We can find f_p and g_p similarly.

Step3 : Weighting

The question about how much of the face curvature should be accumulated at each vertex is very important because different meshes have different resolution at different position. Thus, an appropriate weighting function can help to reduce the error in the curvature approximation significantly. For each face f which is adjacent

to the vertex p , we take the weighting $w_{f,p}$ to be the area of f divided by the squares of the lengths of the two edges that touch the vertex p . The weighting function we use can take care of the different resolution at different location of the mesh and effectively produce more accurate estimation of the curvature, normal and so on.

5.2. Variational method for landmark tracking. Given the principal direction field $\vec{V}(t)$ with smaller eigenvalues on the cortical surface C , we propose a variational method to trace the sulcal landmark curve iteratively, after fixing two anchor points (a & b) on the sulci. Let $\phi : D \rightarrow C$ be the conformal parametrization of C , $\langle \cdot, \cdot \rangle$ to be its Riemannian metric and λ to be its conformal factor. We propose to locate a curve $\vec{c} : [0, 1] \rightarrow C$ with endpoints a and b , that minimizes the following energy functional:

$$E_{principal}(\vec{c}) = \int_0^1 \left| \frac{\vec{c}'}{\sqrt{\langle \vec{c}', \vec{c}' \rangle_M}} - \vec{V} \circ \vec{c} \right|_M^2 dt = \int_0^1 \left| \frac{\vec{\gamma}'}{|\vec{\gamma}'|} - \vec{G}(\vec{\gamma}) \right|^2 dt$$

where $\vec{\gamma} = \vec{c} \circ \phi^{-1} : [0, 1] \rightarrow D$ is the corresponding iteratively defined curve on the parameter domain; $\vec{G}(\vec{\gamma}) = \sqrt{\lambda(\vec{\gamma})}\vec{V}(\vec{\gamma})$; $|\cdot|_M^2 = \langle \cdot, \cdot \rangle_M$ and $|\cdot|$ is the (usual) length defined on D . By minimizing the energy E , we minimize the difference between the tangent vector field along the curve and the principal direction field \vec{v} . The resulting minimizing curve is the curve that is closest to the curve traced along the principal direction. Let:

$$\begin{aligned} \vec{G} &= (G_1, G_2, G_3); \vec{K} = (K_1, K_2, K_3) = \frac{\vec{\gamma}'}{|\vec{\gamma}'|} - \vec{G}(\vec{\gamma}) \\ \vec{L}_1 &= \frac{(1,0,0)}{|\vec{\gamma}'|} - \frac{\gamma'_1 \vec{\gamma}}{|\vec{\gamma}'|^3}; \vec{L}_2 = \frac{(0,1,0)}{|\vec{\gamma}'|} - \frac{\gamma'_2 \vec{\gamma}}{|\vec{\gamma}'|^3}; \vec{L}_3 = \frac{(0,0,1)}{|\vec{\gamma}'|} - \frac{\gamma'_3 \vec{\gamma}}{|\vec{\gamma}'|^3} \end{aligned}$$

Based on the Euler-Lagrange equation, we can locate the landmark curve iteratively using the steepest descent algorithm:

$$\frac{d\vec{\gamma}}{dt} = \sum_{i=1}^3 [K_i \vec{L}_i]' + K_i \nabla G_i$$

(See Appendix)

5.3. Landmark hypothesis by Chan-Vese segmentation. In order to speed up the iterative scheme, we decided to obtain a good initialization by extracting the high curvature regions on the cortical surface using the Chan-Vese (CV) segmentation method [1, 16]. We can extend the CV segmentation on \mathbb{R}^2 to any arbitrary Riemann surface M such as the cortical surface.

Let $\phi : \mathbb{R}^2 \rightarrow M$ be the conformal parametrization of the surface M . We propose to minimize the following energy functional:

$$\begin{aligned} F(c_1, c_2, \psi) &= \int_M (u_0 - c_1)^2 H(\psi) dS \\ &+ \int_M (u_0 - c_2)^2 (1 - H(\psi)) dS \\ &+ \nu \int_M |\nabla_M H(\psi)|_M dS \end{aligned}$$

where $\psi : M \rightarrow \mathbb{R}$ is the level set function and $|\cdot|_M = \sqrt{\langle \cdot, \cdot \rangle}$ and u_0 is the mean curvature function on the cortical surface.

With the conformal parametrization, we have:

$$\begin{aligned} F(c_1, c_2, \psi) &= \int_{\mathbb{R}^2} \lambda(u_0 \circ \phi - c_1)^2 H(\psi \circ \phi) dx dy \\ &+ \int_{\mathbb{R}^2} \lambda(u_0 \circ \phi - c_2)^2 (1 - H(\psi \circ \phi)) dx dy \\ &+ \nu \int_{\mathbb{R}^2} \sqrt{\lambda} |\nabla H(\psi \circ \phi)| dx dy \end{aligned}$$

For simplicity, we let $\zeta = \psi \circ \phi$ and $w_0 = u_0 \circ \phi$. Fixing ζ , we must have:

$$\begin{aligned} c_1(t) &= \frac{\int_{\Omega} w_0 H(\zeta(t, x, y)) \lambda dx dy}{\int_{\Omega} H(\zeta(t, x, y)) \lambda dx dy}, \\ c_2(t) &= \frac{\int_{\Omega} w_0 (1 - H(\zeta(t, x, y))) \lambda dx dy}{\int_{\Omega} (1 - H(\zeta(t, x, y))) \lambda dx dy} \end{aligned}$$

Fixing c_1, c_2 , the Euler-Lagrange equation becomes:

$$\frac{\partial \zeta}{\partial t} = \lambda \delta(\zeta) \left[\nu \frac{1}{\lambda} \nabla \cdot \left(\sqrt{\lambda} \frac{\nabla \zeta}{\|\nabla \zeta\|} \right) - (w_0 - c_1)^2 + (w_0 - c_2)^2 \right]$$

Now, the sulcal landmarks on the cortical surface lie at locations with relatively high curvature. To formulate the CV segmentation, we can consider the intensity term as being defined by the mean curvature. Sulcal locations can then be circumscribed by first extracting out the high curvature regions. Fixing two anchor points inside the extracted region, we can get a good initialization of the landmark curve by looking for a shortest path inside the region that joins the two points. We select two umbilic points as the anchor points. By definition, an *umbilic point* on a manifold is a location at which the two principal curvatures are the same. Therefore, the umbilic points are the 'singularities' of the surface. Also, the umbilic points are the positions where the principal directions are not well-defined. (In other words, $E_{principal}$ is not well defined at these points.) If there are multiple umbilic points are found in one region, we select the two that are furthest apart.

6. Optimization of brain conformal parametrization. In brain mapping research, cortical surface data are often mapped conformally to a parameter domain such as a sphere, providing a common coordinate system for data integration [?, 17, 18]. As an application of our automatic landmark tracking algorithm, we use the automatically labelled landmark curves to generate an optimized conformal mapping on the surface, in the sense that homologous features across subjects are caused to lie at the same parameter locations in a conformal grid. This matching of cortical patterns improves the alignment of data across subjects. This is done by minimizing the compound energy functional $E_{new} = E_{harmonic} + \lambda E_{landmark}$, where $E_{harmonic}$ is the harmonic energy of the parameterization and $E_{landmark}$ is the landmark mismatch energy. Here, automatically traced landmark (continuous) curves are used and the correspondence are obtained using the unit speed reparametrization.

Suppose C_1 and C_2 are two cortical surfaces we want to compare. We let $\phi_1 : C_1 \rightarrow S^2$ be the conformal parameterization of C_1 mapping it onto S^2 . Let $\{p_i : [0, 1] \rightarrow S^2\}$ and $\{q_i : [0, 1] \rightarrow S^2\}$ be the automatic labelled landmark curves, represented on the parameter domain S^2 with unit speed parametrization, for C_1 and C_2 respectively. Let $h : C_2 \rightarrow S^2$ be any homeomorphism from C_2 onto S^2 . We define the landmark mismatch energy of h as: $E_{landmark}(h) =$

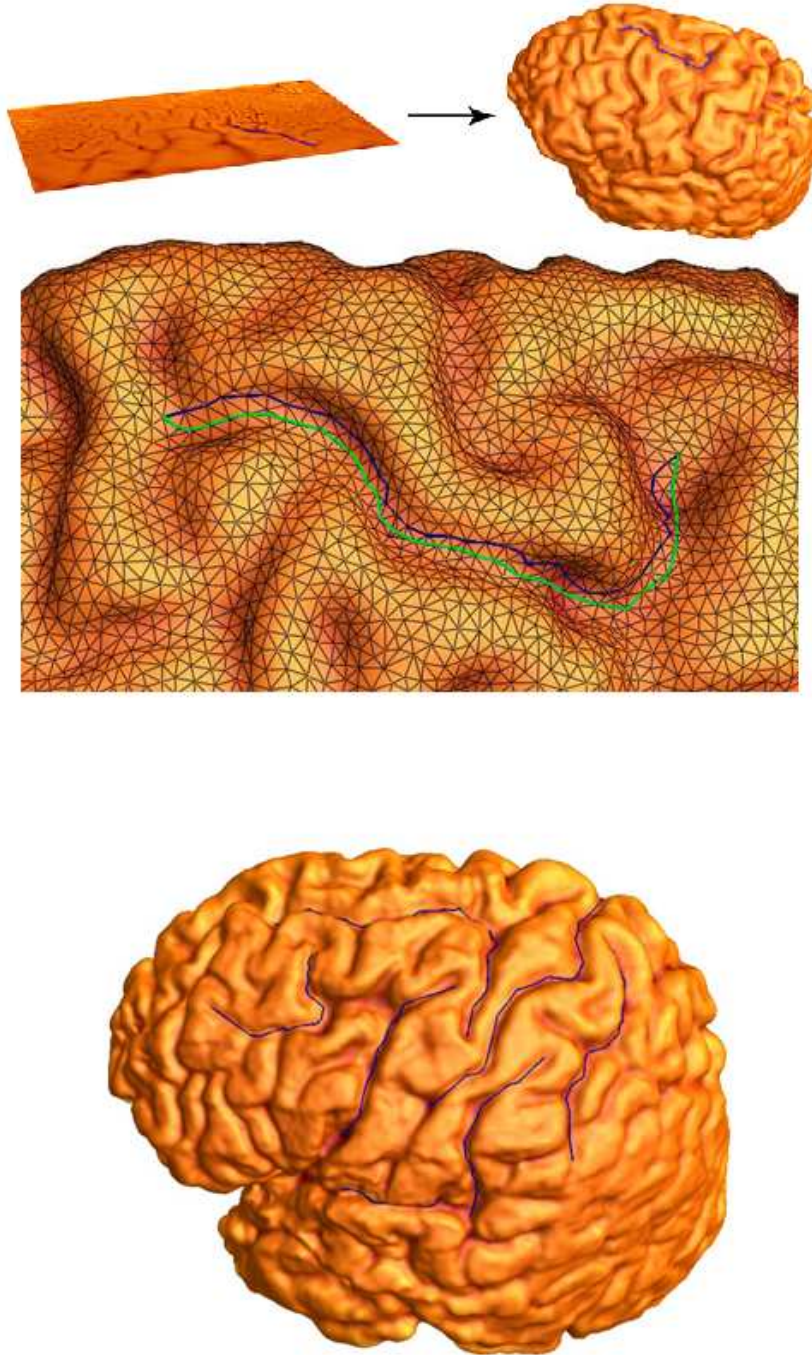


FIGURE 2. Automatic landmark tracking using a variational approach. **Top** : With the global conformal parameterization of the entire cortical surface, we trace the landmark curves on the parameter domain along the edges whose directions are closest to the principal direction field. It gives a good initial guess of the landmark curve (blue curve). The landmark curve is then evolved to a deeper region (green curve) using our variational approach. **Bottom** : Ten sulci landmarks are automatically traced using our algorithm.

$1/2 \sum_{i=1}^n \int_0^1 \|h(q_i(t)) - \phi_1(p_i(t))\|^2 dt$, where the norm represents distance on the sphere. By minimizing this energy functional, the Euclidean distance between the corresponding landmarks on the sphere is minimized.

7. Experimental results. In one experiment, we tested our automatic landmark tracking algorithm on a set of 40 left hemisphere cortical surfaces extracted from brain MRI scans, acquired from normal subjects at 1.5 T (on a GE Signa scanner). In our experiments, 10 major sulcal landmarks (central/precentral) were automatically located on cortical surfaces.

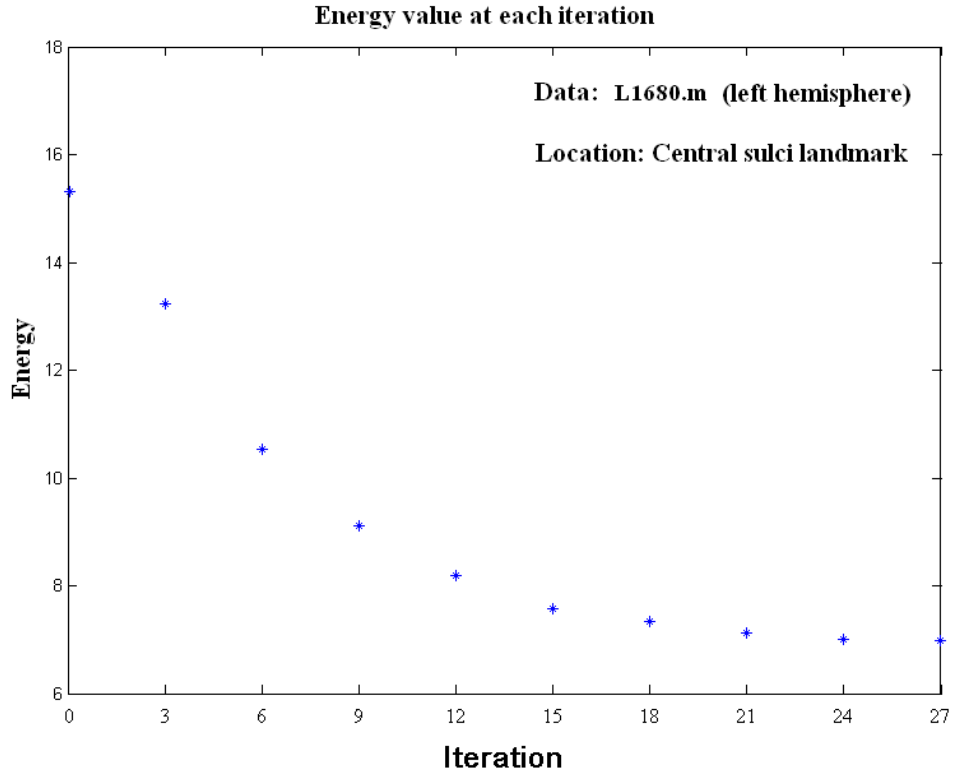
Figure 5(Top), shows how we can effectively locate the initial landmark guess areas on the cortical surface using the Chan-Vese segmentation. Notice that the contour evolved to the deep sulcal region. In Figure 5(Bottom), we locate the umbilic points in each sulcal region, which are chosen as the anchor points.

Our variational method to locate landmark curves is illustrated in Figure 2. With the initial guess given by the Chan-Vese model (we choose the two extreme points in the located area as the anchor points), we trace the landmark curves iteratively based on the principal direction field. In Figure 2 (left), we trace the landmark curves on the parameter domain along the edges whose directions are closest to the principal direction field. The corresponding landmark curves on the cortical surface is shown. Figure 2 (left) shows how the curve evolves to a deeper sulcal region with our iterative scheme. In Figure 2 (right), ten sulci landmarks are located using our algorithm. Our algorithm is quite efficient with the good initial guess using the CV-model. (See Fig 3 Top)

To compare our automatic landmark tracking results with the manually labeled landmarks, we measured the Euclidean distance $E_{difference}$ (on the parameter domain) between the automatically and manually labelled landmark curves. Figure 3(Bottom) shows the value of the Euclidean distance $E_{difference} = \int_0^1 \|\vec{c}_{principal}(t) - \vec{c}_{manual}(t)\|^2 dt$ between the automatically and manually labelled landmark curves at different iterations for different landmark curves. The two landmark curves are unit-speed parametrized, denoted by $\vec{c}_{principal}(t)$ and $\vec{c}_{manual}(t)$ respectively. The manually-labeled sulci landmarks are manually labeled directly on the brain surface by neuroscientists. Note that the value becomes smaller as the iterations proceed. This means that the automatically labeled landmark curves more closely resemble those defined manually as the iterations continues.

Figure 4 illustrates the application of our automatic landmark tracking algorithm. We illustrated our idea of the optimization of conformal mapping using the automatically traced landmark curves. Figure 4 (A) and (B) show two different cortical surfaces being mapped conformally to the sphere. Notice that the alignment of the sulci landmark curves are not consistent. In Figure 4 (C), the same cortical surface in (B) is mapped to the sphere using our method. Notice that the landmark curves closely resemble to those in (A), meaning that the alignment of the landmark curves are more consistent with our algorithm.

To visualize how well our algorithm can improve the alignment of the important sulci landmarks is, we took average surface of the 15 cortical surfaces by using the optimized conformal parametrization algorithm [16]. Figure 4(D), (E) and (F) shows the average surface (for N=15 subjects) based on the optimized conformal re-parametrization using the variational approach. Except in (F), where no landmarks were defined automatically, the major sulcal landmarks are remarkably well



Difference between the two landmarks is measured by:

$$E_{difference} = \int_0^1 \|\vec{c}_{principal}(t) - \vec{c}_{manual}(t)\|^2 dt$$

L1627.m	Central	Pre-central	Post-central
Iteration 0	1.28	1.31	1.27
Iteration 30	0.21 ↓ 83.6%	0.22 ↓ 83.2%	0.21 ↓ 83.5%

L1680.m	Central	Pre-central	Post-central
Iteration 0	1.33	1.35	1.26
Iteration 30	0.24 ↓ 82.0%	0.28 ↓ 79.3%	0.26 ↓ 79.4%

FIGURE 3. **Top** : The value of $E_{principal}$ at each iteration is shown. Energy reached its steady state with 30 iterations, meaning that our algorithm is efficient using the CV model as the initialization. **Bottom** : Numerical comparison between automatic labelled landmarks and manually labelled landmarks by computing the Euclidean distance $E_{difference}$ (on the parameter domain) between the automatically and manually labelled landmark curves, which are unit-speed parametrized. These manually-labeled sulci landmarks are manually labeled directly on the brain surface by neuroscientists.

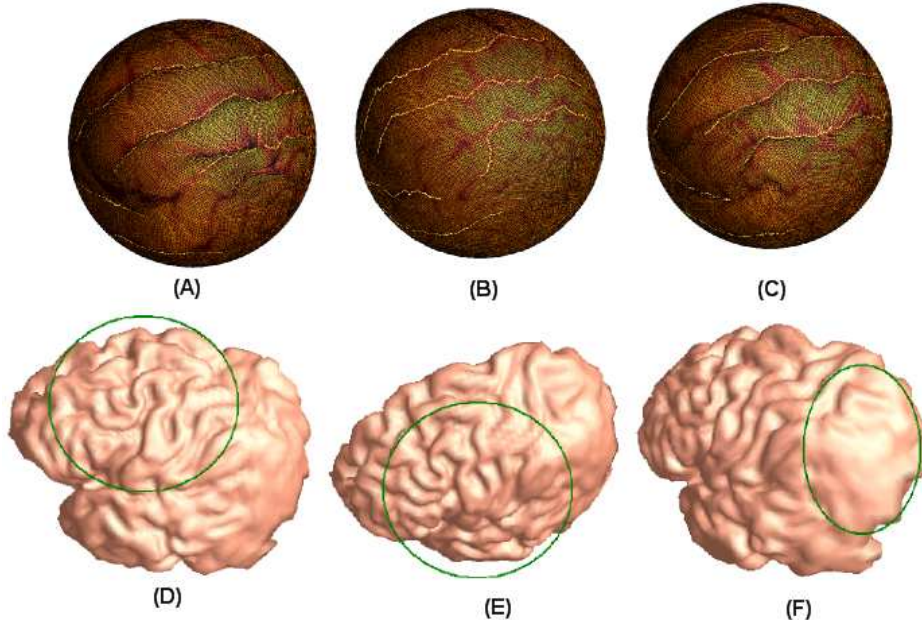


FIGURE 4. Optimization of brain conformal mapping using automatic landmark tracking. In (A) and (B), two different cortical surfaces are mapped conformally to the sphere. The corresponding landmark curves are aligned inconsistently on the spherical parameter domain. In (C), we map the same cortical surface of (B) to the sphere using our algorithm. Note that the alignment of the landmark curves are much more consistent with the those in (A). (D), (E), (F) shows the average surface (for $N=15$ subjects) based on the optimized conformal re-parametrization using the variational approach. Except in (F), where no landmarks were defined automatically, the major sulcal landmarks are remarkably well defined, even in this multi-subject average.

defined, even in this multi-subject average. As shown in (D) and (E), sulci landmarks are clearly preserved inside the green circle where landmarks were defined automatically. In (F), the sulci landmarks are averaged out inside the green circle where no landmarks were defined. This suggests that our algorithm can help by improving the alignment of major anatomical features in the cortex. Further validation work, of course, would be necessary to assess whether this results in greater detection sensitivity in computational anatomy studies of the cortex, but the greater reinforcement of features suggests that landmark alignment error is substantially reduced, and this is one major factor influencing signal detection in multi-subject cortical studies.

8. Conclusion and future work. In this paper, we propose a variational method to automatically trace landmark curves on cortical surfaces, based on the principal directions. To accelerate the iterative scheme, we initialize the curves by extracting high curvature regions using Chan-Vese segmentation. This involves solving a PDE

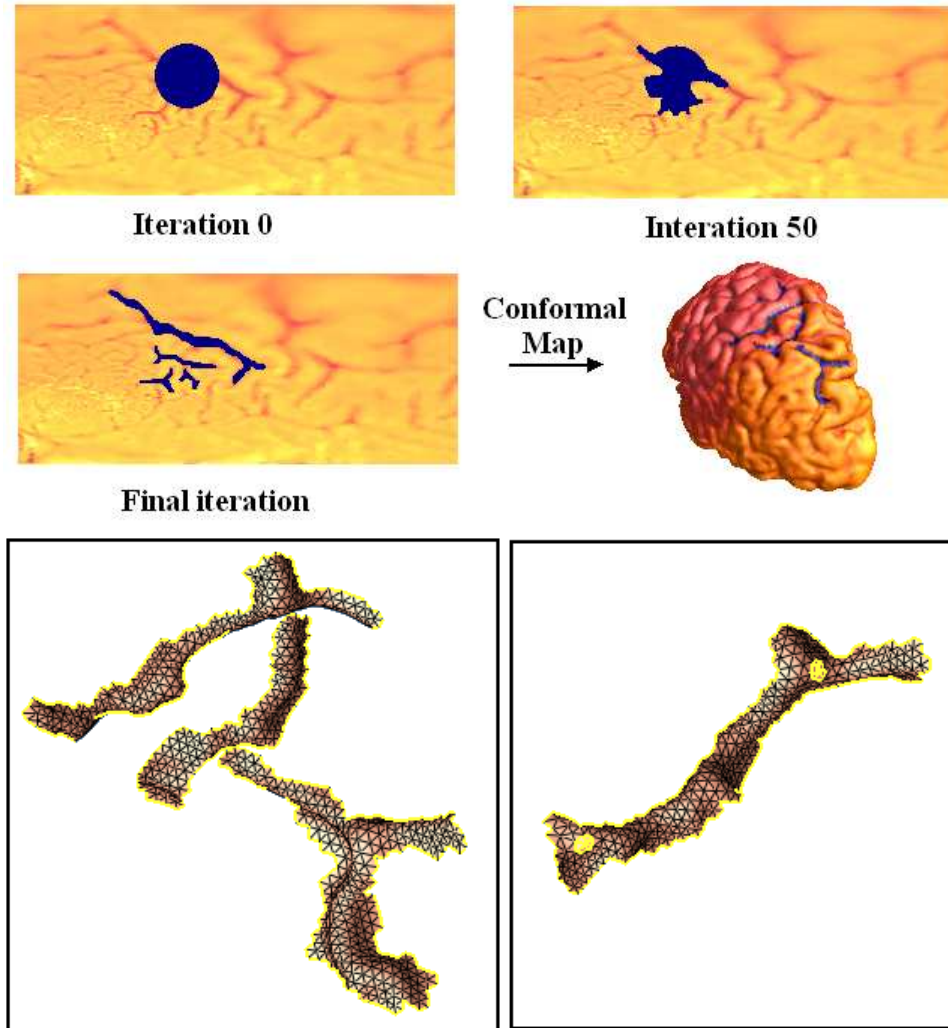


FIGURE 5. **Top** :Sulcal curve extraction on the cortical surface by Chan-Vese segmentation. We consider the intensity term as being defined by the mean curvature. Sulcal locations can then be circumscribed by first extracting out the high curvature regions.**Bottom** : Umbilic points are located on each sulci region, which are chosen as the end points of the landmark curves.

on the cortical manifold. The landmark curves detected by our algorithm closely resembled those labeled manually. Finally, we use the automatically labeled landmark curves to create an optimized brain conformal mapping, which matches important anatomical features across subjects. Surface averages from multiple subjects show that our computed maps can consistently align key anatomic landmarks. In the

future, we will perform more quantitative analysis of our algorithm's performance and quantifying improved registration, across multiple subjects, on a regional basis.

9. Acknowledgment. This work was supported in part by the National Institutes of Health through the NIH Roadmap for Medical Research, grant U54 RR021813 entitled Center for Computational Biology (CCB). Additional support was provided by the NIH/NCCR resource grant P41 RR013642; National Science Foundation (NSF) under Contract DMS-0610079 and ONR Contract N0014-06-1-0345. The work was performed while T. Chan was on leave at the National Science Foundation as Assistant Director of the Directorate for Mathematics. P. Thompson is also supported by the National Institute for Biomedical Imaging and Bioengineering, the National Center for Research Resources, the National Institute for Neurological Disorders and Stroke, National Institute on Aging, and the National Institute for Child Health and Development (EB01651, RR019771, AG016570, NS049194, and HD050735 to P. Thompson.)

APPENDIX

A. The energy $E_{principal}$ is Decreasing. $\frac{dE_{principal}}{ds}|_{s=0}(\vec{\gamma} + s\vec{u})$

$$\begin{aligned}
&= \int_0^1 \frac{d}{ds} \Big|_{s=0} \left| \frac{\vec{\gamma}' + s\vec{u}'}{|\vec{\gamma}' + s\vec{u}'|} - \vec{G}(\vec{\gamma} + s\vec{u}) \right|^2 dt \\
&= \int_0^1 \left(\frac{\vec{\gamma}'}{|\vec{\gamma}'|} - \vec{G}(\vec{\gamma}) \right) \cdot \left[\frac{\vec{u}'}{|\vec{\gamma}'|} - \frac{\vec{\gamma}'(\vec{\gamma}' \cdot \vec{u}')}{|\vec{\gamma}'|^3} - \vec{G}'(\vec{\gamma}) \cdot \vec{u} \right] dt \\
&= \int_0^1 \left(\frac{\vec{\gamma}'}{|\vec{\gamma}'|} - \vec{G}(\vec{\gamma}) \right) \cdot \left[\frac{\vec{u}'}{|\vec{\gamma}'|} - \frac{\vec{\gamma}'(\vec{\gamma}' \cdot \vec{u}')}{|\vec{\gamma}'|^3} - \vec{G}'(\vec{\gamma}) \cdot \vec{u} \right] dt \\
&= - \int_0^1 \sum_{i=1}^3 \{ [K_i \vec{L}_i] + K_i \nabla G_i \} \cdot \vec{u} < 0
\end{aligned}$$

if we let $\vec{u} = \sum_{i=1}^3 \{ [K_i \vec{L}_i] + K_i \nabla G_i \}$.

(Here, G_i, K_i, L_i are defined as in Section 4.3)

Thus, the energy $E_{principal}$ is decreasing.

REFERENCES

- [1] Vese, L., Chan, T., *Multiphase level set framework for image segmentation using the mumford and shah model*, International Journal of Computer Vision, **50** (2002), 271–293.
- [2] Tao, X., Prince, J., Davatzikos, C., *Using a statistical shape model to extract sulcal curves on the outer cortex of the human brain*, IEEE TMI, **21** (2002), 513–524.
- [3] Lohmann, G., Kruggel, F., von Cramon, D., *Automatic detection of sulcal bottom lines in mr images of the human brain*, IPMI, **1230** (1997), 368–374.
- [4] Zeng, X., Staib, L., Schultz, R., Win, L., Duncan, J., *A new approach to 3d sulcal ribbon finding from mr images*, 3rd MICCAI, (1999).
- [5] Kao, C., Hofer, M., Sapiro, G., Stern, J., Rottenberg, D., *A geometric method for automatic extraction of sulcal fundi*, IEEE Intl. Symp. Biomedical Imaging, From Nano to Macro, (2006), 1168–1171.
- [6] Gu, X., Wang, Y., Chan, T.F., Thompson, P.M., Yau, S.T., *Genus zero surface conformal mapping and its application to brain surface mapping*, IEEE Trans. Med. Imag., **23** (2004), 949–958.
- [7] Wang, Y., Lui, L.M., Chan, T.F., Thompson, P.M., *Optimization of brain conformal mapping with landmarks*, in “Med. Image Comp. Comput.-Assist. Intervention, Proceedings,” Part II (2005), 675–683.
- [8] Glaunès, J., Vaillant, M., Miller, M., *Landmark matching via large deformation diffeomorphisms on the sphere*, J. Maths. Imaging and Vision, **20** (2004), 179–200.
- [9] Leow, A., Yu, C., Lee, S., Huang, S., Protas, H., Nicolson, R., Hayashi, K., Toga, A., Thompson, P., *Brain structural mapping using a novel hybrid implicit/explicit framework based on the level-set method*, NeuroImage, **24** (2005), 910–927.
- [10] Thompson, P., Woods, R., Mega, M., Toga, A., *Mathematical/computational challenges in creating population-based brain atlases*, Human Brain Mapping, **9** (2000), 81–92.

- [11] Schoen, R., Yau, S., “Lectures on Harmonic Maps,” International Press, 1997.
- [12] Cipolla, R., Giblin, P.J., “Visual Motion of Curves and Surfaces,” Cambridge University Press, 2000.
- [13] Gu, X., Yau, S., “Global Conformal Surface Parameterization” ACM Symp on Geom. Processing, 2003.
- [14] Wang, Y., Gu, X., Hayashi, K.M., Chan, T.F., Thompson, P.M., Yau, S.T., *Surface parameterization using Riemann surface structure*, in “10th IEEE Intl Conf. on Computer Vision,” Beijing, China, (2005) 1061–1066.
- [15] Rusinkiewicz, S., *Estimating curvatures and their derivatives on triangle meshes*, Symp. on 3D Data Processing, Vis., and Trans, (2004).
- [16] Lui, L., Wang, Y., Chan, T.F., *Solving pdes on manifolds using global conference parametrization*, VLSM, ICCV, (2005).
- [17] Drury, H., Essen, D.V., Corbetta, M., Snyder, A., *Surface-based analyses of the human cerebral cortex*, in “Brain Warping,” Academic Press, 1999.
- [18] Fischl, B., Sereno, M., Tootell, R., Dale, A., *High-resolution intersubject averaging and a coordinate system for the cortical surface*, in “Human Brain Mapping,” **8** (1999), 272–284.

Received September 2006; revised January 2007.

E-mail address: malmlui@math.ucla.edu

E-mail address: ylwang@math.ucla.edu

E-mail address: chan@math.ucla.edu

E-mail address: thompson@loni.ucla.edu